Ab initio description of multipolar responses in superfluid and deformed nuclei at finite temperature: application to dipole modes in ^{56}Fe

Y. Beaujeault-Taudière,[1,2] M. Frosini,[3,4] J.-P. Ebran,[1,2] T. Duguet,[4,5] R. Roth,[6,7] and V. Somà[4]

[1] *CEA, DAM, DIF, 91297 Arpajon, France*
[2] *Université Paris-Saclay, CEA, Laboratoire Matière en Conditions Extrêmes, 91680 Bruyères-le-Châtel, France*
[3] *CEA, DEN, IRESNE, DER, SPRC, 13108 Saint-Paul-lès-Durance, France*
[4] *IRFU, CEA, Université Paris-Saclay, 91191 Gif-sur-Yvette, France*
[5] *KU Leuven, Department of Physics and Astronomy, Instituut voor Kern- en Stralingsfysica, 3001 Leuven, Belgium*
[6] *Institut für Kernphysik, Technische Universität Darmstadt, 64289 Darmstadt, Germany*
[7] *Helmholtz Forschungsakademie Hessen für FAIR, GSI Helmholtzzentrum, 64289 Darmstadt, Germany*

(Dated: March 28, 2022)

Ab initio approaches to the nuclear many-body problem have seen their reach considerably extended over the past decade. However, collective excitations have rarely been addressed due to the prohibitive cost of solving the corresponding equations of motion. Here, a numerically efficient method to compute ab initio multipolar responses of superfluid and deformed nuclei at finite temperature is presented. As a pilot application, the electromagnetic dipolar responses in ^{56}Fe based on chiral two- and three-body nuclear interactions are computed over the temperature interval $k_BT \in [0, 4]$ MeV, where k_B is the Boltzmann constant. This development directly opens the way to the systematic ab initio study of multipolar excitations at finite temperature in light and medium-mass nuclei.

Introduction. – Atomic nuclei host a vast diversity of behaviours, for which a comprehensive description poses several formal and technical difficulties. In particular, nuclear vibrational excitations, ranging from non-collective (e.g., pygmy) [1, 2] to highly collective modes (the so-called giant resonances) [3–5], constitute a long-term challenge for the quantum many-body problem formulated in terms of nucleonic degrees of freedom. Their description is especially demanding for ab initio approaches where only sporadic calculations have been performed so far, in spite of the ever-increasing applicability of such methods across the nuclear chart [6].

Namely, early attempts to compute multipolar response functions from an ab initio standpoint made use of the random phase approximation (RPA) [7] and its quasiparticle extension (QRPA) [8]. More recent calculations have been performed either via the coupled cluster (CC) [9–12] or the self-consistent Green's function (SCGF) approach [13], however limited to dipole responses of closed-shell systems. The extension of such methods to open-shell nuclei is highly non-trivial because of the associated prohibitive numerical cost. As a result, ab initio nuclear responses are currently out of reach for the large majority of nuclei, even in the light and medium-mass sectors.

In the context of empirical nuclear energy density functionals, a novel scheme to solve the (Q)RPA equations was proposed a few years ago in Refs. [14, 15]. This approach, coined as the (quasiparticle) finite amplitude method ((Q)FAM), replaces the intensive calculation and diagonalisation of the QRPA matrix by a set of non-linear equations of similar dimension to that of the static Hartree-Fock-Bogoliubov (HFB) mean-field approach it builds upon. The QFAM has proven to be a very efficient tool to obtain electric [16–19] and charge-exchange [20, 21] strength functions, as well as to determine collective inertia [22, 23], quasiparticle-vibration coupling [24], discrete eigenmodes [25] and sum rules [26]. Very recently, the method has been extended to the finite temperature QFAM (FT-QFAM) [27].

On the ab initio side, novel efforts have been made to extend structure calculations to deformed and superfluid nuclei [28–31]. These developments are well suited to be combined with FAM-type algorithms. In this letter, the first ab initio implementation of the FT-QFAM is presented and applied to investigate the electromagnetic dipole response of the doubly open-shell, medium-mass ^{56}Fe nucleus. The resulting method is (i) based on full two- and three-body interactions rooted in quantum chromodynamics (QCD), (ii) applicable to doubly-magic, singly-magic and doubly open-shell nuclei and (iii) characterised by a favourable scaling with mass number. As a result, it opens the path to systematic ab initio computations of multipolar responses at zero and finite temperature across a large span of the nuclear chart.

In the long term, first-principles calculations of electromagnetic nuclear response functions could provide valuable input for astrophysical simulations. In this sense, the ^{56}Fe nucleus acts as a representative of Fe-group nuclei that are of astrophysical relevance. First, the photodisintegration of Fe-group nuclei plays an important role during the last stages of hydrostatic burning in massive stars and during their explosion in type-II supernovae [32]. Second, the propagation of ultra-high-energy cosmic rays depends on the interactions of Fe-group nuclei with photons from the cosmic microwave background [33, 34].

In the following, after describing the basics of the FT-QFAM and the numerical setting, results based on a family of ab initio nuclear Hamiltonians are reported. First, ground-state thermodynamic properties are investigated via finite temperature HFB (FT-HFB) theory. Next, finite-temperature isovector dipole electric and magnetic strength distributions are computed and analysed by applying the FT-QFAM on top of the FT-HFB calculation.

Formalism. – The present approach starts with a FT-HFB calculation to access the ground state and its thermal excitations [35–37]. Diagonalising the mean-field FT-HFB Hamiltonian $\mathcal{H}_0$ via the Bogoliubov transformation

$$\mathcal{W}_0 \equiv \begin{pmatrix} U & V^* \\ V & U^* \end{pmatrix}, \tag{1}$$

with (U, V) being the corresponding quasi-particle (qp) eigenvectors, one obtains

$$\mathcal{H}_0 = \begin{pmatrix} E & 0 \\ 0 & -\bar{E} \end{pmatrix} \; ; \; \mathcal{R}_0 = \begin{pmatrix} f & 0 \\ 0 & 1-\bar{f} \end{pmatrix}, \tag{2}$$

where $\mathcal{R}_0$ denotes the FT-HFB generalised density matrix and E the diagonal matrix of qp eigenenergies. The quantity $f \equiv (1+e^{\beta E})^{-1}$ characterises the associated Fermi-Dirac factors, with $\beta \equiv (k_{\mathrm{B}}T)^{-1}$ and k_{B} the Boltzmann constant. Up to trivial permutations that are presently discarded for simplicity, $\bar{E} = E$ and $\bar{f} = f$.

Nuclear excited states are accessed by perturbing the ground-state via an external probe represented here by a generic one-body operator $\mathcal{F}$ written in the qp eigenbasis of $\mathcal{H}_0$ as

$$\mathcal{F} \equiv \begin{pmatrix} F^{11} & F^{20} \\ F^{02} & F'^{11} \end{pmatrix}. \tag{3}$$

The FT-QFAM is obtained by linearising the corresponding finite temperature time-dependent HFB (FT-TDHFB) formalism. In frequency representation, one obtains [38, 39] the equation of motion

$$\omega\delta\mathcal{R} = [\mathcal{H}_0, \mathcal{F}+\delta\mathcal{R}] + [\delta\mathcal{H}, \mathcal{R}_0], \tag{4}$$

where ω denotes the excitation energy whereas $\delta\mathcal{H}$ and $\delta\mathcal{R}$ characterise the first-order fluctuations on top of $\mathcal{H}_0$ and $\mathcal{R}_0$, respectively, that are parameterised in the qp eigenbasis through

$$\delta\mathcal{H}(\omega) \equiv \mathcal{W}_0^\dagger \begin{pmatrix} \delta h & \delta\Delta^{(+)} \\ -\delta\Delta^{(-)*} & -\delta h^T \end{pmatrix} \mathcal{W}_0 \equiv \begin{pmatrix} H^{11} & H^{20} \\ H^{02} & H'^{11} \end{pmatrix}; \tag{5a}$$

$$\delta\mathcal{R}(\omega) \equiv \mathcal{W}_0^\dagger \begin{pmatrix} \delta\rho & \delta\kappa^{(+)} \\ -\delta\kappa^{(-)*} & -\delta\rho^T \end{pmatrix} \mathcal{W}_0 \equiv \begin{pmatrix} W & X \\ Y & Z \end{pmatrix}, \tag{5b}$$

where δh, $\delta\Delta^{(+)}$ and $\delta\Delta^{(-)*}$ ($\delta\rho$, $\delta\kappa^{(+)}$ and $\delta\kappa^{(-)*}$) denote the oscillating normal and anomalous mean fields (densities) expressed in the underlying single-particle basis. Matrices X and Y define the usual forward and backward linear response amplitudes, whereas W (Z) describes transitions among positive (negative) energy states only.

Inverting Eq. (4), the components of the generalised density fluctuation are given in the qp basis by

$$X_{\mu\nu} = -\frac{H^{20}_{\mu\nu} + F^{20}_{\mu\nu}}{E_\mu + \bar{E}_\nu - \omega_\gamma}(1 - \bar{f}_\nu - f_\mu), \tag{6a}$$

$$Y_{\mu\nu} = -\frac{H^{02}_{\mu\nu} + F^{02}_{\mu\nu}}{\bar{E}_\mu + E_\nu + \omega_\gamma}(1 - \bar{f}_\mu - f_\nu), \tag{6b}$$

$$W_{\mu\nu} = -\frac{H^{11}_{\mu\nu} + F^{11}_{\mu\nu}}{E_\mu - E_\nu - \omega_\gamma}(f_\nu - f_\mu), \tag{6c}$$

$$Z_{\mu\nu} = -\frac{H'^{11}_{\mu\nu} + F'^{11}_{\mu\nu}}{\bar{E}_\mu - \bar{E}_\nu + \omega_\gamma}(\bar{f}_\nu - \bar{f}_\mu), \tag{6d}$$

where the excitation frequency has been shifted into the complex plane, $\omega_\gamma \equiv \omega + i\gamma$, to avoid hitting the poles that lie on the real axis in case the system is stable under the action of $\mathcal{F}$. Solving Eq. (6) efficiently requires to compute, with mild numerical effort, the induced fields δh, $\delta\Delta^{(+)}$ and $\delta\Delta^{(-)*}$ that are functionals of $\delta\rho$, $\delta\kappa^{(+)}$ and $\delta\kappa^{(-)*}$. In this process, the oscillating mean fields are explicitly linearised with respect to the induced density fluctuations, which eventually leads to expressing them as static-like HFB mean fields. However, care must be taken of the fact that the fluctuating fields and densities possess fewer symmetries than their static counterpart, making their computation more involved than in the initial static FT-HFB step.

Equations (5) and (6) form a closed set to be solved iteratively for each frequency ω_γ. The physical quantity of interest, i.e., the FT-QFAM strength function characterising the response of the system to the perturbation, is computed as

$$S(\mathcal{F}, \omega_\gamma) = \mathrm{Tr}\{\mathcal{F}^\dagger \delta\mathcal{R}(\omega_\gamma)\}. \tag{7}$$

Note that the finite value of γ introduces a Lorentzian smearing in the strength calculated with Eq. (7). Eventually, for a multipole transition operator $\mathcal{F}_{JK}$ characterised by total angular momentum J and its projections $K = -J, \ldots, +J$ onto the z axis, the imaginary part of the strength containing the dissipative contribution to the response amounts to

$$S_J(\omega) \equiv -\frac{1}{\pi}\sum_{K=-J}^{J} \mathrm{Im}\{S(\mathcal{F}_{JK}, \omega_\gamma)\}. \tag{8}$$

Noticeably, the FT-QFAM strength can eventually be used to extract individual FT-QRPA eigenvalues $(\omega_\gamma)_k$ and eigenvectors $(W, X, Y, Z)_k$, as well as the so-called sum rules, via an extension of the method proposed in Refs. [25, 26]; see Ref. [40] for details.

Computational setting. – Numerical applications are performed using a family of Hamiltonians [41] containing two- and three-nucleon interactions derived from chiral effective field theory (χEFT) [42, 43] at next-to-leading-order (NLO), N^{2}LO and N^{3}LO. These Hamiltonians are made suitable for nuclear structure calculations by a subsequent similarity renormalisation group (SRG) transformation down to a flow parameter $\lambda_{\rm srg} = 1.88$ fm^{-1}; see Refs. [41, 44] for details about the determination of the low-energy constants and the SRG evolution. In order to allow for a systematic study of the convergence of observables with the order of the χEFT expansion, the calculations at N^{2}LO and N^{3}LO are accompanied by an assessment of the associated uncertainty; see Refs. [40, 43, 45, 46] for details.

The treatment of three-nucleon interactions is a challenge in ab initio nuclear structure calculations, and here is made possible via the procedure described in Ref. [47]. While this treatment is strictly exact in FT-HFB and FT-QFAM calculations of non-superfluid spherical nuclei, it becomes quasi exact whenever the system deforms and/or is superfluid, as is presently the case for ^{56}Fe; see Ref. [47] for details.

The eigenbasis of a spherical harmonic oscillator Hamiltonian is employed as a computational basis to expand one-, two- and three-body operators. The truncated basis is characterised by the maximum oscillator quanta $\mathrm{e}_{\rm max} = 10$ and the frequency $\hbar\Omega = 16$ MeV. In the three-body Hilbert space, the basis is further truncated according to $\mathrm{e}_{\rm 3max} = 14 < 3\,\mathrm{e}_{\rm max}$. All observables at HFB level (energy, radii, deformation) are converged to a subpercent accuracy with respect to basis size and oscillator frequency. Strength functions and integrated moments do not vary by more than 3% between 8 and 10 oscillator shells.

Ground-state thermodynamic properties. – Ground-state thermodynamic properties are obtained via a FT-HFB calculation that finds ^{56}Fe to be prolate with a zero-temperature quadrupole deformation parameter $\beta_2(T = 0) = 0.31 \pm 0.01$. Figure 1 displays the evolution of thermal excitations $E^*(T) \equiv E(T) - E(0)$, the entropy[1] $S(T) \equiv -(\partial F/\partial T)$, the heat capacity $C_v(T) \equiv T\partial S/\partial T$, and the quadrupole deformation $\beta_2(T)$ with temperature. Results are compared to those obtained for a two-component free fermion gas (FFG) by adapting the formulae of Ref. [48], using $\rho_{\rm n} = \rho_{\rm p} = 0.08$ fm^{-3} and $m_n = m_p = 939$ MeV.

While the excitation energy and entropy both roughly exhibit the quadratic and linear dependencies expected for a FFG, the heat capacity allows us to identify a second-order phase transition[2]. As corroborated by the bottom panel of Fig. 1, the phase transition corresponds to a restoration of the spherical symmetry at the critical temperature.

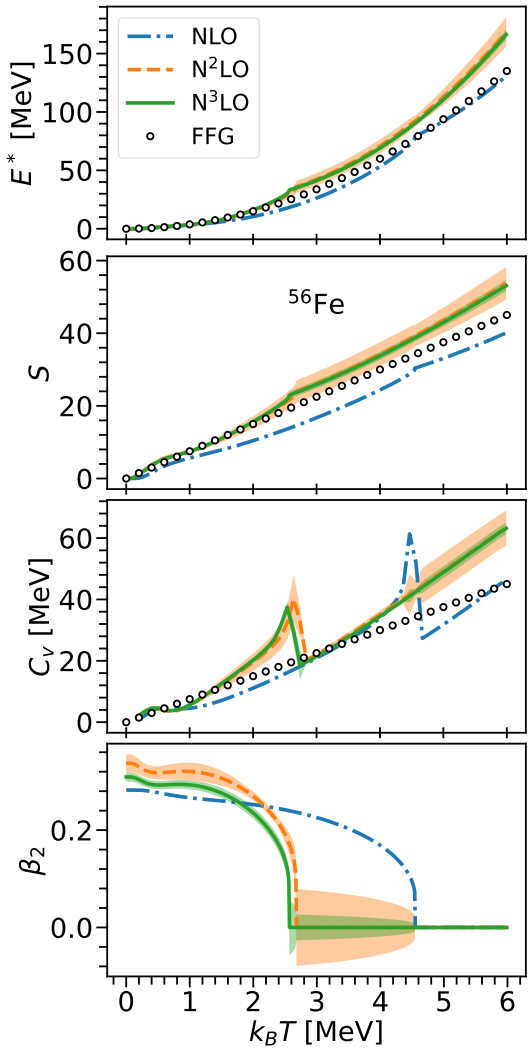

FIG. 1. FT-HFB ground-state thermodynamic properties of ^{56}Fe computed as a function of the temperature at NLO, N^{2}LO and N^{3}LO. From top to bottom panels: thermal excitation energy, entropy, heat capacity and quadrupolar deformation.

As visible from all panels, the FT-HFB results change significantly when going from NLO to N^{2}LO. In particular, the critical temperature decreases from $k_BT_c = 4.5$ MeV to $k_BT_c = 2.7$ MeV. Contrarily, results change very little when going from N^{2}LO to N^{3}LO, e.g. the critical temperature is only lowered by 0.1 MeV, reaching $k_BT_c = 2.6 \pm 0.2$ MeV. Furthermore, N^{3}LO results are quite consistently and systematically within the uncer-

[1] $F = E - TS$ denotes here the Helmholtz free energy.

[2] While the heat capacity does not diverge in Fig. 1, increasing the number of mesh points over the temperature interval would result in such a divergence of C_v. Further adding quantum collective fluctuations to the present description would eventually smear out such a divergence.

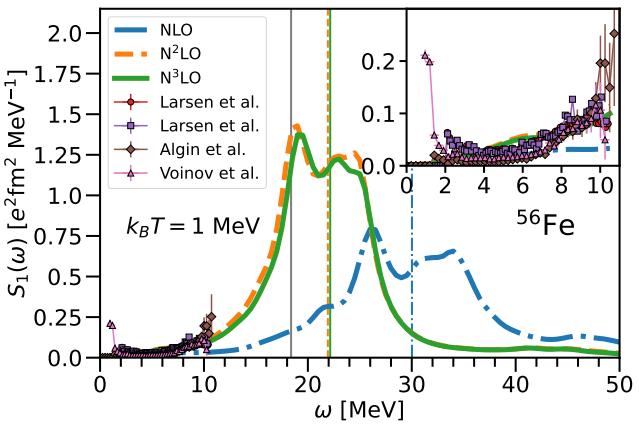

FIG. 2. Theoretical electromagnetic isovector dipole ($E1 + M1$) response computed in ^{56}Fe at NLO, N^{2}LO and N^{3}LO for $k_BT = 1$ MeV and $\gamma = 1.5$ MeV. The corresponding mean energies are indicated by vertical lines. The low-energy part [49–51] and mean value [57] of the experimental strength are also provided.

tainty of N^{2}LO results, the uncertainty of the N^{3}LO results themselves being significantly reduced compared to N^{2}LO ones. These features indicate that the systematic uncertainty on ground-state thermodynamic properties of ^{56}Fe associated with the chiral expansion of the nuclear Hamiltonian is small by the time N^{3}LO is reached.

Isovector dipole excitations. – Measured and predicted total electromagnetic ($E1 + M1$) isovector dipole (IVD) response functions are displayed in Fig. 2. The experimental IVD $\gamma-$strength functions [49–51] were extracted using the Oslo method [52, 53], from which the temperature of the final state was estimated to be approximately $k_BT = 1$ MeV. The theoretical IVD strength distributions are, therefore, computed at that temperature. The comparison of theoretical excitation strength functions with de-excitation measurements is meaningful, given that the Brink-Axel hypothesis has been shown to hold within experimental uncertainties in ^{56}Fe [54–56].

The convergence of the results with respect to the chiral expansion order follows a pattern similar to the one observed for ground-state properties. In particular, the proximity of N^{2}LO and N^{3}LO results indicates a good convergence[3], which is in fact systematically observed for other multipolarities and nuclei. Eventually, the N^{3}LO strength function agrees well with available experimental

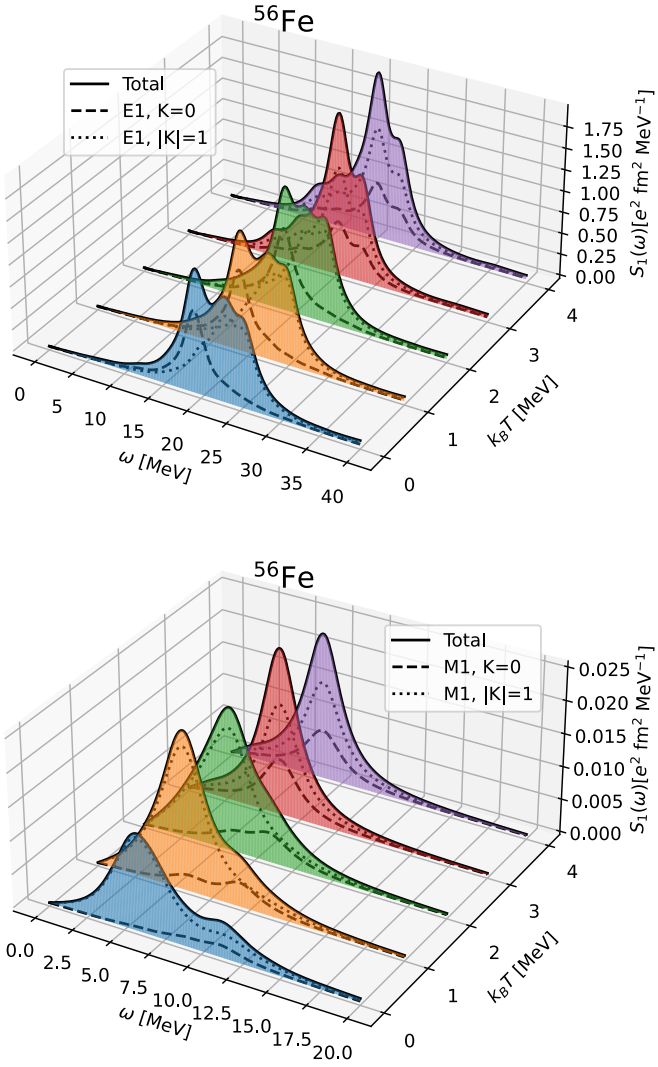

FIG. 3. Finite-temperature $E1$ (top) and $M1$ (bottom) responses of ^{56}Fe. The N^{3}LO Hamiltonian is employed. The FAM amplitudes are smeared using $\gamma = 1.5$ MeV.

values over the interval $\omega \in [2, 10]$ MeV.

Next, the evolution of the N^{3}LO IVD strength, decomposed into its $K = 0$ and $|K| = 1$ electric and magnetic components[4], is investigated in Figs. 3 and 4 over the temperature interval $k_BT \in [0, 4]$ MeV. At zero temperature, the maxima of $K = 0$ and $|K| = 1$ components are shifted apart as a result of the intrinsic deformation of ^{56}Fe ground-state. This feature provides both the electric and magnetic responses with a two-peak structure. While both $|K|$ components are equally important in the electric response, the $|K| = 1$ component largely dominates the magnetic one.

[3] The discrepancy between N^{2}LO and N^{3}LO results at a given excitation energy is due to the FT-HFB qp spectrum being slightly different, which in turn displaces the energy of the resonances. While these shifts, albeit very small, magnify the change (at most 10%) at a given excitation frequency due to the sharpness of the peaks, they are strongly suppressed in integrated quantities such as the total photo-emission cross section [47] or the mean excitation energy that changes by less than one percent.

[4] Due to the axial symmetry imposed in the calculation, $K = 1$ and $K = -1$ responses contribute identically.

The increasing temperature induces two competing processes. On the one hand, the temperature smears out the Fermi-Dirac factors associated with the zero-temperature mean-field, with the effect of globally increasing the matter radius R of the system. In schematic models of the giant dipole resonance in spherical nuclei of Goldhaber and Teller (GT) [58] or Steinwedel, Jensen and Jensen (SJJ) [59], this effect induces a decrease of the peak energy according to $R^{-1/2}$ (GT) and R^{-1} (SJJ) laws, respectively. This effect is indeed qualitatively visible for the $|K| = 1$ component of the electric response in Fig. 4. On the other hand, the temperature additionally generates a collective transformation of the mean-field at play, driving the system from being deformed at zero temperature to being spherical beyond T_c (see lower panel of Fig. 1). Because the $K = 0$ electric component operates along the symmetry axis, the change from prolate to spherical shape leads to an effective decrease of the matter distribution in this direction. As a result of these two competing effects, the E_{10} mean energy undergoes almost no evolution up to T_c until it merges with the decreasing E_{11}, initially located at higher energy. The merging beyond T_c of the initially different $K = 0$ and $|K| = 1$ responses is precisely the fingerprint of the phase transition associated with the restoration of spherical symmetry. Beyond that point, the main resonance keep evolving downwards, whereas the further increase of thermally excitations enhance the dipole strength at $\omega \lesssim 12\,\mathrm{MeV}$.

Magnetic modes being located at much lower energies than electric ones, they bear greater sensitivity to thermal excitations that dominate their evolution. As a result, the mean $K = 0$ and $|K| = 1$ excitation energies continuously decrease until their merging at T_c.

Eventually, the IVD response is mostly driven by the electric modes, resulting in a mean excitation energy of about 22 MeV at $k_BT = 1$ MeV. This value is higher than the experimental centroid, located at 18.4 MeV. Present results indicate that uncertainties associated with the chiral expansion of the nuclear Hamiltonian and the truncation of the computational basis are not responsible for this 20% discrepancy. This calls for questioning uncertainty sources that have not been investigated in this first study. While one may inquire the error associated with discarded terms beyond three-body operators in the SRG evolution of the Hamiltonian, many-body correlations beyond QRPA are most likely responsible and must eventually be considered. In doubly closed-shell nuclei, such correlations have been shown to typically lower the centroid by several MeVs in addition to fragmenting the strength distribution [60, 61].

Conclusions. – This letter presents the first ab initio description of giant resonances at finite temperature in mid-mass nuclei with a method handling simultaneously pairing correlations and deformation, i.e., allowing the indiscriminate study of doubly closed-shell, singly open-shell and doubly open-shell nuclei. Utilising the finite amplitude method to solve quasi-particle random phase approximation equations on the basis of two- and three-nucleon interactions derived from a low-energy effective theory of quantum chromodynamics unlocks the possibility to calculate the collective response of nuclei to various types of excitations in an ab initio framework, while guaranteeing a much gentler numerical scaling than traditional eigenvalue approaches. Applying the method to a representative nucleus of astrophysical interest, i.e., the doubly open-shell ^{56}Fe nucleus, the effects of the temperature on the isovector dipole strength distribution have been scrutinised and the potential for systematic applications highlighted.

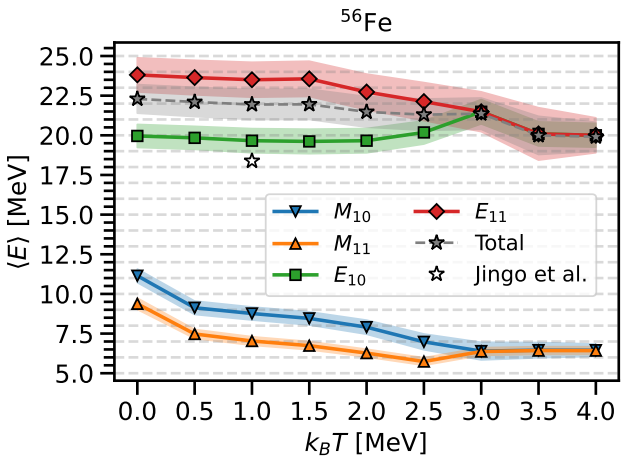

FIG. 4. Thermal evolution of the mean excitation energies for the different dipoles modes in ^{56}Fe. The white star denotes the experimental measurement of [57], whereas the grey stars represent the calculated average energy of the sum of all four dipole modes. The N^{3}LO Hamiltonian is employed and the QFAM amplitudes are smeared using $\gamma = 1.5$ MeV.

Acknowledgements. – We would like to thank S. Goriely for interesting discussions and for providing the experimental strength functions, and A. Porro for cross-checking our calculations. Calculations were performed using HPC resources from GENCI-TGCC (Contracts No. A0090507392 and A0110513012). RR acknowledges support by the DFG through SFB 1245 (Project ID 279384907) and the BMBF through Verbundprojekt 05P2021 (ErUM-FSP T07, Contract No. 05P21RDFNB).

[1] N. Paar, D. Vretenar, E. Khan, and G. Colò, Reports on Progress in Physics **70**, 691 (2007).
[2] D. Savran, T. Aumann, and A. Zilges, Progress in Particle and Nuclear Physics **70**, 210 (2013).

[3] W. Bothe and W. Gentner, Zeitschrift für Physik **106**, 236 (1937).
[4] N. BOHR, Nature **141**, 326 (1938).
[5] M. N. Harakeh and A. van der Woude, *Giant Resonances: Fundamental High-Frequency Modes of Nuclear Excitation* (Oxford University Press, 2001).
[6] L. Coraggio, S. Pastore, and C. Barbieri, Front. in Phys. **8**, 626976 (2021), arXiv:2101.07915 [nucl-th].
[7] N. Paar, P. Papakonstantinou, H. Hergert, and R. Roth, Phys. Rev. C **74**, 014318 (2006).
[8] H. Hergert, P. Papakonstantinou, and R. Roth, Phys. Rev. C **83**, 064317 (2011).
[9] S. Bacca, N. Barnea, G. Hagen, M. Miorelli, G. Orlandini, and T. Papenbrock, Phys. Rev. C **90**, 064619 (2014), arXiv:1410.2258 [nucl-th].
[10] M. Miorelli, S. Bacca, N. Barnea, G. Hagen, G. R. Jansen, G. Orlandini, and T. Papenbrock, Phys. Rev. C **94**, 034317 (2016), arXiv:1604.05381 [nucl-th].
[11] M. Miorelli, S. Bacca, G. Hagen, and T. Papenbrock, Phys. Rev. C **98**, 014324 (2018), arXiv:1804.01718 [nucl-th].
[12] F. Bonaiti, S. Bacca, and G. Hagen, (2021), arXiv:2112.08210 [nucl-th].
[13] F. Raimondi and C. Barbieri, Phys. Rev. C **99**, 054327 (2019), arXiv:1811.07163 [nucl-th].
[14] T. Nakatsukasa, T. Inakura, and K. Yabana, Phys. Rev. C **76**, 024318 (2007).
[15] P. Avogadro and T. Nakatsukasa, Phys. Rev. C **84**, 014314 (2011).
[16] T. Inakura, T. Nakatsukasa, and K. Yabana, Phys. Rev. C **80**, 044301 (2009).
[17] M. Stoitsov, M. Kortelainen, T. Nakatsukasa, C. Losa, and W. Nazarewicz, Phys. Rev. C **84**, 041305 (2011).
[18] M. Kortelainen, N. Hinohara, and W. Nazarewicz, Phys. Rev. C **92**, 051302 (2015).
[19] T. Oishi, M. Kortelainen, and N. Hinohara, Phys. Rev. C **93**, 034329 (2016).
[20] M. T. Mustonen, T. Shafer, Z. Zenginerler, and J. Engel, Phys. Rev. C **90**, 024308 (2014).
[21] E. M. Ney, J. Engel, T. Li, and N. Schunck, Phys. Rev. C **102**, 034326 (2020).
[22] N. Hinohara, Phys. Rev. C **92**, 034321 (2015).
[23] K. Washiyama, N. Hinohara, and T. Nakatsukasa, Phys. Rev. C **103**, 014306 (2021).
[24] E. Litvinova and Y. Zhang, Phys. Rev. C **104**, 044303 (2021).
[25] N. Hinohara, M. Kortelainen, and W. Nazarewicz, Phys. Rev. C **87**, 064309 (2013).
[26] N. Hinohara, M. Kortelainen, W. Nazarewicz, and E. Olsen, Phys. Rev. C **91**, 044323 (2015).
[27] A. Ravlić, Y. F. Niu, T. Nikšić, N. Paar, and P. Ring, (2021), 10.1103/PhysRevC.104.064302, arXiv:2108.08702 [nucl-th].
[28] J. M. Yao, B. Bally, J. Engel, R. Wirth, T. R. Rodríguez, and H. Hergert, Phys. Rev. Lett. **124**, 232501 (2020).
[29] M. Frosini, T. Duguet, J.-P. Ebran, and V. Somà, (2021), arXiv:2110.15737 [nucl-th].
[30] M. Frosini, T. Duguet, J.-P. Ebran, B. Bally, T. Mongelli, T. R. Rodríguez, R. Roth, and V. Somà, (2021), arXiv:2111.00797 [nucl-th].
[31] M. Frosini, T. Duguet, J.-P. Ebran, B. Bally, H. Hergert, T. R. Rodríguez, R. Roth, J. M. Yao, and V. Somà, (2021), arXiv:2111.01461 [nucl-th].
[32] M. Arnould and S. Goriely, Progress in Particle and Nuclear Physics **112**, 103766 (2020).
[33] E. Khan, S. Goriely, D. Allard, E. Parizot, T. Suomijärvi, A. Koning, S. Hilaire, and M. Duijvestijn, Astroparticle Physics **23**, 191 (2005).
[34] Allard, D., Parizot, E., Olinto, A. V., Khan, E., and Goriely, S., A&A **443**, L29 (2005).
[35] K. Tanabe, K. Sugawara-Tanabe, and H. Mang, Nuclear Physics A **357**, 20 (1981).
[36] A. L. Goodman, Nuclear Physics A **352**, 30 (1981).
[37] J. L. Egido and P. Ring, J. Phys. G **19**, 1 (1993).
[38] P. Ring and P. Schuck, *The nuclear many-body problem* (Springer-Verlag, New York, 1980).
[39] H. M. Sommermann, Annals of Physics **151**, 163 (1983).
[40] Y. Beaujeault-Taudière, *Study of the multipolar excitations in cold and hot, deformed and superfluid systems with the method of finite amplitudes*, Theses, Université Paris-Saclay (2021).
[41] T. Hüther, K. Vobig, K. Hebeler, R. Machleidt, and R. Roth, Physics Letters B **808**, 135651 (2020).
[42] S. Weinberg, Physica A: Statistical Mechanics and its Applications **96**, 327 (1979).
[43] D. R. Entem, R. Machleidt, and Y. Nosyk, Phys. Rev. C **96**, 024004 (2017).
[44] T. Hüther, *Families of Chiral Two- plus Three-Nucleon Interactions for Accurate Nuclear Structure Studies*, Ph.D. thesis, Technische Universität, Darmstadt (2021).
[45] E. Epelbaum, H. Krebs, and U.-G. Meißner, The European Physical Journal A **51**, 53 (2015).
[46] S. Binder, A. Calci, E. Epelbaum, R. J. Furnstahl, J. Golak, K. Hebeler, T. Hüther, H. Kamada, H. Krebs, P. Maris, U.-G. Meißner, A. Nogga, R. Roth, R. Skibiński, K. Topolnicki, J. P. Vary, K. Vobig, and H. Witała (LENPIC Collaboration), Phys. Rev. C **98**, 014002 (2018).
[47] M. Frosini, T. Duguet, B. Bally, Y. Beaujeault-Taudière, J. P. Ebran, and V. Somà, Eur. Phys. J. A **57**, 151 (2021), arXiv:2102.10120 [nucl-th].
[48] L. Landau and E. Lifshitz, in *Statistical Physics (Third Edition)*, edited by L. Landau and E. Lifshitz (Butterworth-Heinemann, Oxford, 1980) third edition ed., pp. 158–190.
[49] A. Voinov, E. Algin, U. Agvaanluvsan, T. Belgya, R. Chankova, M. Guttormsen, G. E. Mitchell, J. Rekstad, A. Schiller, and S. Siem, Phys. Rev. Lett. **93**, 142504 (2004).
[50] E. Algin, U. Agvaanluvsan, M. Guttormsen, A. C. Larsen, G. E. Mitchell, J. Rekstad, A. Schiller, S. Siem, and A. Voinov, Phys. Rev. C **78**, 054321 (2008).
[51] A. C. Larsen, N. Blasi, A. Bracco, F. Camera, T. K. Eriksen, A. Görgen, M. Guttormsen, T. W. Hagen, S. Leoni, B. Million, H. T. Nyhus, T. Renstrøm, S. J. Rose, I. E. Ruud, S. Siem, T. Tornyi, G. M. Tveten, A. V. Voinov, and M. Wiedeking, Phys. Rev. Lett. **111**, 242504 (2013).
[52] A. Schiller, L. Bergholt, M. Guttormsen, E. Melby, J. Rekstad, and S. Siem, Nuclear Instruments and Methods in Physics Research Section A: Accelerators, Spectrometers, Detectors and Associated Equipment **447**, 498 (2000).
[53] J. E. Midtbø, F. Zeiser, E. Lima, A.-C. Larsen, G. M. Tveten, M. Guttormsen, F. L. B. Garrote, A. Kvellestad, and T. Renstrøm, "A new software implementation of the oslo method with rigorous statistical uncertainty propagation," (2021), arXiv:1904.13248 [physics.comp-ph].

[54] A. V. Voinov, S. M. Grimes, U. Agvaanluvsan, E. Algin, T. Belgya, C. R. Brune, M. Guttormsen, M. J. Hornish, T. Massey, G. E. Mitchell, J. Rekstad, A. Schiller, and S. Siem, Phys. Rev. C **74**, 014314 (2006).

[55] A. C. Larsen, M. Guttormsen, N. Blasi, A. Bracco, F. Camera, L. C. Campo, T. K. Eriksen, A. Görgen, T. W. Hagen, V. W. Ingeberg, B. V. Kheswa, S. Leoni, J. E. Midtbø, B. Million, H. T. Nyhus, T. Renstrøm, S. J. Rose, I. E. Ruud, S. Siem, T. G. Tornyi, G. M. Tveten, A. V. Voinov, M. Wiedeking, and F. Zeiser, Journal of Physics G: Nuclear and Particle Physics **44**, 064005 (2017).

[56] M. D. Jones, A. O. Macchiavelli, M. Wiedeking, L. A. Bernstein, H. L. Crawford, C. M. Campbell, R. M. Clark, M. Cromaz, P. Fallon, I. Y. Lee, M. Salathe, A. Wiens, A. D. Ayangeakaa, D. L. Bleuel, S. Bottoni, M. P. Carpenter, H. M. Davids, J. Elson, A. Görgen, M. Guttormsen, R. V. F. Janssens, J. E. Kinnison, L. Kirsch, A. C. Larsen, T. Lauritsen, W. Reviol, D. G. Sarantites, S. Siem, A. V. Voinov, and S. Zhu, Phys. Rev. C **97**, 024327 (2018).

[57] M. Jingo, E. Z. Buthelezi, J. Carter, G. R. J. Cooper, R. W. Fearick, S. V. Förtsch, C. O. Kureba, A. M. Krumbholz, P. von Neumann-Cosel, R. Neveling, and et al., The European Physical Journal A **54** (2018), 10.1140/epja/i2018-12664-5.

[58] M. Goldhaber and E. Teller, Phys. Rev. **74**, 1046 (1948).

[59] H. Steinwedel, J. H. D. Jensen, and P. Jensen, Phys. Rev. **79**, 1019 (1950).

[60] P. Papakonstantinou and R. Roth, Phys. Lett. B **671**, 356 (2009).

[61] P. Papakonstantinou and R. Roth, Phys. Rev. C **81**, 024317 (2010), arXiv:0910.1674 [nucl-th].